ICIC Express Letters
Volume **18**, Number **5**, May **2024**

ICIC International ©2024 ISSN 1881-803X
pp. **493–501**

HIGH-ORDER DISTURBANCE OBSERVER BASED ON GRNN FOR QUAV ANTI-DISTURBANCE CONTROL

Xiaolong Wang, Shuyi Shao* and Hongzhen Guo

College of Automation Engineering
Nanjing University of Aeronautics and Astronautics
No. 29, Jiangjun Avenue, Nanjing 211100, P. R. China
{ xiaolongw; guohongzhen }@nuaa.edu.cn
*Corresponding author: shaosy@nuaa.edu.cn

Received August 2023; accepted October 2023

Abstract. *Aiming at the wind and turbulence faced by the inspection quadrotor unmanned aerial vehicles flying in large buildings, this paper remodels the disturbance and designs a high-order disturbance observer (HODO) to ensure that the quadrotor can resist wind disturbance. Firstly, the disturbance is modeled into linear and nonlinear types. Then, the generalized regression neural network (GRNN) is designed to estimate the nonlinear part. Then, the HODO is designed to estimate the errors introduced by the linear and nonlinear parts and use the Lyapunov function to prove the system's stability. Finally, a numerical simulation is designed to verify the feasibility of the algorithm.*
Keywords: High-order disturbance observer (HODO), Generalized regression neural network (GRNN), Discrete time, Nonlinear disturbance

1. **Introduction.** Quadrotor unmanned aerial vehicles (QUAVs) have been widely used in environments unsuitable for human work [1]. Due to its small size, simple structure, and easy deployment [2], it has been widely used in power inspection [3], emergency rescue [4], and fire detection [5]. Inspecting the facade of large buildings also needs to work in the same human-unfriendly working environment. Generally speaking, when QUAVs flying in the complex buildings group, due to the small space between them, there may be continuous gusts and turbulence, which will affect the regular inspection work of the QUAVs [6]. Therefore, designing and implementing a robust anti-disturbance control system has attracted many researchers.

A lot of valuable work on the high-order disturbance observer (HODO) has been carried out in recent years [7-10]. Sarsembayev et al. designed a disturbance observer-based control (DOBC) method for permanent magnet synchronous motor (PMSM) drives [11]. It has been proved that the proposed observer evaluated the system by fewer speed errors and faster response. As for the quadrotor, Ahmed et al. combined the HODO with sliding model control (SMC) to obtain the desired tracking performance [12]. Considering the matched and mismatched disturbances, extensive simulations were conducted and proved that the method was effective. Generalized regression neural network (GRNN) is an application form of radius basis function neural network (RBFNN), which is mainly used for nonlinear function estimation under discrete time conditions. A nonlinear control method combined with GRNN and SMC was used to find practical solutions for controlling nonlinear dynamic systems [13]. The proposed design changed the GRNN to an online adaptive controller without pretraining which means the system can obtain nonlinear dynamic online.

The above work has demonstrated the efficient application of GRNN in nonlinear function estimation, stability control design, etc., which provides great inspiration for the

DOI: 10.24507/icicel.18.05.493

method in this paper. Motivated by the above discussion, together with the HODO and GRNN, an anti-disturbance control method is designed in this paper. The main contributions are listed in the following.

a) Aiming at the continuous wind and turbulence from the environment, the disturbance system is remodeled in an unknown nonlinear way to be observed.

b) A four-layer adaptive GRNN to fit the nonlinear dynamic of disturbance is designed. Due to the lack of training data, an adaptive parameter update law is developed and applied to the network to achieve the purpose of self-learning updates.

c) Together with this network structure, a new nth-order disturbance observer is designed to estimate the linear part of the disturbance. The Lyapunov function is used to prove that the whole system is uniformly ultimately bounded (UUB). Furthermore, the numerical simulation proved the effectiveness. The rest of this node is organized as follows. The problem formulation and preliminaries are given in Section 2. The HODO and the GRNN are designed in Section 3. The numerical simulation and results are presented in Section 4. Finally, the conclusion is drawn in Section 5.

2. **Problem Statement and Preliminaries.** The quadrotor is always considered as a classic nonlinear system. According to its working environment and considering the states of each order, the model can be defined into a linear state space function at time k in the discrete-time domain with sample time T through small disturbance linearization, which can be expressed in the following form:

$$\begin{cases} x_{k+1} = Ax_k + Bu_k + d_k \\ y_k = Cx_k \end{cases} \tag{1}$$

where $x_k \in \mathbb{R}^6$ represents the state of the system consisting of the position and velocity of the quadrotor. $u_k \in \mathbb{R}^4$ and $y_k \in \mathbb{R}^6$ are defined as the input and output signals, respectively. $A \in \mathbb{R}^{6\times6}$, $B \in \mathbb{R}^{6\times4}$, $x_k \in \mathbb{R}^{6\times n_d}$ are matrices related to linearized system, and n_d is the dimension of disturbance dynamic d_k. The disturbance in this paper can be designed in the form of

$$\begin{cases} \xi_{k+1} = A_d\xi_k \\ d_k = C_d\xi_k + D(x_k) \end{cases} \tag{2}$$

where $\xi_k \in \mathbb{R}^{n_d}$ represents the state of the disturbance, and $A_d, C_d \in \mathbb{R}^{n_d\times n_d}$ are the linear constant matrices. $D(x_k)$ represents a nonlinear matrix function related to the states of the quadrotor.

Remark 2.1. *The working environment considered in this paper is a narrow space between large buildings, where the disturbance type is mostly wind disturbance. Wind disturbances generally include continuously excited gusts and turbulence, which can be represented as linear and nonlinear exogenous systems, respectively. The linear part is modeled as a system (A_d, C_d). Suppose that the effect of wind disturbances on QUAVs as an energy field, the disturbance received by the quadrotor in the wind field is related to its position and flight speed, so the nonlinear part is represented in the form of $D(x_k)$ in the model related to the quadrotor states.*

The following assumptions and lemmas are presented and will be used in the subsequent developments to facilitate the anti-disturbance control system design.

Assumption 2.1. [14]. *The states and outputs of the quadrotor plant are all measurable.*

Assumption 2.2. *The disturbance and its state are unmeasurable due to the real environment. However, they are assumed to be bounded.*

Assumption 2.3. [10]. *All derivatives of the disturbance exist, and all derivatives are bounded, which means $d^{(1)}, d^{(2)}, \ldots, d^{(n)}$ all exist and are bounded.*

Assumption 2.4. [10]. *The reference trajectory r and its derivatives exist and are bounded.*

Lemma 2.1. *As the turbulence type of wind disturbance in a continuous time zone can be approximated by RBFNN with a bounded error, the same type of disturbance $D(x_k)$ can also be expressed by a class of generalized regression neural network as follows:*

$$D(z) = \Phi_k^T \Theta(z) + \epsilon_k \tag{3}$$

where $z = [z_1, z_2, \ldots, z_p]^T \in \mathbb{R}^p$ represents the input vector of the GRNN [13], *$\Phi_k \in \mathbb{R}^{L_N \times N}$ is the weight matrix of GRNN, L_N, N represent the neuron layers in pattern layer and the input dimension, and $\Theta(z) = [\Theta_1(z), \Theta_2(z), \ldots, \Theta_q(z)]^T$ is a function vector representing the four layers and q neurons of GRNN. There always exists the optimal weight value Φ_k^* of GRNN which is given by*

$$\Phi_k^* = \arg\min_{\Phi \in \mathbb{D}} \left[\sup_{z \in \mathbb{S}} |D(z, \Phi_k) - D(z)| \right] \tag{4}$$

where $\mathbb{D}$ is a bounded close set that represents the valid set of the parameter of GRNN, and $\mathbb{S} \in \mathbb{R}^q$ is an allowable set of the input vector. Introducing the optimal weight matrix, (3) yields

$$D(z) = \Phi_k^* \Theta(z) + \epsilon_k^* \tag{5}$$

where $|\epsilon_k^*| \leq \bar{\epsilon}$ is the optimal approximation error and $\bar{\epsilon} > 0$ is the upper bound of the error.

3. Main Results.

In this section, an anti-disturbance control method will be designed for unknown wind and turbulence based on the high-order disturbance observer and generalized regression neural network.

3.1. Design of generalized regression neural network.

In order to better estimate the dynamic of unknown nonlinear disturbances, a GRNN with a four-layer network is used to design a nonlinear fitting estimator, including the input layer, the pattern layer, the summation layer, and the output layer.

Input layer: The input of this layer is also the input of the network, which is defined as $x_k \in \mathbb{R}^{N \times 1}$. The output is expressed as the Euclidean distance between the input value at the current moment and the mean value of all previous input state values, which can be defined as the following form

$$D_k = \mathrm{d}(M_k, x_k) \tag{6}$$

where $M_k = \begin{bmatrix} \mu_k^{11} & \ldots & \mu_k^{1N} \\ \vdots & & \vdots \\ \mu_k^{L_N 1} & \ldots & \mu_k^{L_N N} \end{bmatrix} \in \mathbb{R}^{L_N \times N}$, $\mathrm{d}(m, n)$ represents the Euclidean distance calculation function. Furthermore, the update law of μ_k^{ln} in M_k is defined as

$$\mu_k^{ln} = \frac{k-1}{k} \mu_{k-1}^{ln} + \frac{1}{k} x_{k_n} \tag{7}$$

where x_{k_n} represents the nth component of the input state x_k at time k.

Pattern layer: The input of this layer is $D_k \in \mathbb{R}^{N \times 1}$. The output of this layer is the calculation result of redesigned Gaussian kernel function. The data transmission is maintained in the form of a full connection between the two layers, where the kernel function defining the neuron is

$$\theta_k^{lc} = e^{\frac{-\left(D_k^l\right)^2}{2\sigma^2}}, \quad c = 1, \ldots, C \tag{8}$$

where C is the number of neurons. Further design $\theta^l = \left[\theta^{l1}, \theta^{l2}, \ldots, \theta^{lC}\right] \in \mathbb{R}^{1\times C}$ and the output of this layer $\Theta_k = \left[\Theta_k^1, \Theta_k^2, \ldots, \Theta_k^{L_N}\right]^T$ can be defined as

$$\Theta_k^l = \frac{\sum_{c=1}^{C} \theta_k^{lc}}{C} \tag{9}$$

Summation layer: The input of this layer is $\Theta_k^l \in \mathbb{R}^{L\times 1}$. The outputs of this layer contain $S_D \in \mathbb{R}$ representing the algebraic sum of the elements in the input vector and $S_N \in \mathbb{R}^{N\times 1}$ standing for weighted input vector. They can be defined as

$$\begin{cases} S_{D_k} = \sum_{l=1}^{L_N} \Theta_k^l \\ S_{N_k} = \hat{\Phi}_k^T \Theta_k \end{cases} \tag{10}$$

Output layer: The input of this layer is $S_D \in \mathbb{R}$ and $S_N \in \mathbb{R}^{N\times 1}$, and the final output of the whole network can be defined as

$$\hat{D}(x_k) = \hat{\Phi}_k^T \Theta_n(x_k) + \epsilon_k \tag{11}$$

where $\Theta_n(x_k) = \frac{\Theta_k}{\sum_{l=1}^{L_N} \Theta_k^l}$. And the updating law of the weight can be expressed as

$$\hat{\Phi}_{k+1} = \hat{\Phi}_k - \gamma \Theta_n(x_k) \tilde{y}_k \tag{12}$$

where γ is defined as the learning rate, and the output error is defined as $\tilde{y}_k = y_k - r_k$. Based on the kernel function, we can know that there exists a border that satisfied $\|\Theta_n(x_k)\| \le \mu$, $\mu > 0$.

3.2. **Design of high-order disturbance observer.** According to the form of the disturbance dynamic we modeled and the GRNN designed above, we can know that introducing GRNN to estimate the nonlinear dynamics of disturbance will inevitably introduce unpredictable deviations; at the same time, the state ξ_k of the disturbance dynamics is still unmeasured. Therefore, this paper introduces an HODO to observe the state of disturbance dynamics.

DOB 0: First of all, the 1st-order observer can be designed as follows:

$$\begin{cases} \hat{\xi}_k = z_k + L x_k \\ z_{k+1} = -L\left(A x_k + B u_k + \hat{d}_k\right) + A_d \hat{\xi}_k \\ \hat{d}_k = C_d \hat{\xi}_k + \hat{D}(x_k) \end{cases} \tag{13}$$

where z_k is the auxiliary variable. We can further get the derivative of the state $\hat{\xi}_k$ in the following form:

$$\begin{aligned} \hat{\xi}_{k+1} &= z_{k+1} + L x_{k+1} \\ &= -L\left(A x_k + B u_k + \hat{d}_k\right) + A_d \hat{\xi}_k + L(A x_k + B u_k + d_k) \\ &= A_d \hat{\xi}_k + L\left(C_d \hat{\xi}_k + \tilde{D}(x_k)\right) \end{aligned} \tag{14}$$

where $\tilde{D}(x_k) := D(x_k) - \hat{D}(x_k) = \tilde{\Phi}_k^T \Theta_n(x_k)$. Furthermore, we can obtain the estimation error and its derivative in the form of

$$\tilde{\xi}_{k+1} = \xi_{k+1} + \hat{\xi}_{k+1} = (A_d - L C_d)\tilde{\xi}_k - L\tilde{D}(x_k) \tag{15}$$

As we know from the previous discussion, $\tilde{D}(x_k)$ is bounded. If an appropriate L is selected to satisfy $A_d - LC_d \le 0$, then $\tilde{\xi}_k$ can ensure that it eventually converges to a bounded area related to the bound of $\tilde{D}(x_k)$, which verifies the effectiveness of the design.

DOB *i*: Based on the designed principle of **DOB 0**, we can generalize the design of HODO to counteract the influence of the boundary of $\tilde{D}(x_k)$ from GRNN on the observer. For $i = 0, 1, 2, \ldots, n-1$, we can get the disturbance $d_k^{(i)}$ and $\hat{\xi}_k^{(i)}$ to any ith-order as the following form:

$$\begin{cases} \hat{\xi}_k^{(i)} = z_k^i + L_i x_k \\ z_{k+1}^i = -L_i \left(Ax_k + Bu_k + \hat{d}_k \right) + A_d \hat{\xi}_k^{(i)} - \hat{\xi}_k^{(i+1)} \\ \hat{d}_k^{(i)} = C_d \hat{\xi}_k^{(i)} + \hat{D}(x_k) \end{cases} \tag{16}$$

where z_k^i is defined as the auxiliary variable. As described before, we can obtain the derivative of the disturbance state and the estimation error in the form of

$$\begin{cases} \hat{\xi}_{k+1}^{(i)} = A_d \hat{\xi}_k^{(i)} + L_i C_d \hat{\xi}_k + L_i \tilde{D}(x_k) - \hat{\xi}_k^{(i+1)} \\ \tilde{\xi}_{k+1}^{(i)} = A_d \tilde{\xi}_k^{(i)} - L_i C_d \hat{\xi}_k - L_i \tilde{D}(x_k) + \hat{\xi}_k^{(i+1)} \end{cases} \tag{17}$$

DOB *n*: Unlike the ith-order disturbance observer, the nth-order disturbance observer no longer includes the highest-order term to ensure final convergence. Therefore, the nth-order disturbance observer can be defined as the following form:

$$\begin{cases} \hat{\xi}_{k+1}^{(n)} = z_k^n + L_n x_k \\ z_{k+1}^n = -L_n \left(Ax_k + Bu_k + \hat{d}_k \right) + A_d \hat{\xi}_k^{(n)} \\ \hat{d}_k^{(n)} = C_d \hat{\xi}_k^{(n)} + \hat{D}(x_k) \end{cases} \tag{18}$$

where z_k^n is defined as the auxiliary variable and we can have the final estimation error of the nth-order disturbance observer in the form of

$$\tilde{\xi}_{k+1}^{(n)} = A_d \tilde{\xi}_k^{(n)} - L_n C_d \hat{\xi}_k - L_n \tilde{D}(x_k) \tag{19}$$

If we manage all these observers together, a $(n+1)$-dimensional extended vector of observer error can be defined as $\Xi_k = \left[\tilde{\xi}_k, \tilde{\xi}_k^{(1)}, \tilde{\xi}_k^{(2)}, \ldots, \tilde{\xi}_k^{(n)} \right]^T \in \mathbb{R}^{n+1}$ which includes the **DOB 0**. Furthermore, we can obtain its difference.

$$\begin{aligned} \Xi_{k+1} &= \left[\tilde{\xi}_{k+1}, \tilde{\xi}_{k+1}^{(1)}, \tilde{\xi}_{k+1}^{(2)}, \ldots, \tilde{\xi}_{k+1}^{(n)} \right]^T \\ &= \begin{bmatrix} A_d - L_0 C_d & I & 0 & \ldots & 0 \\ -L_1 C_d & A_d & I & \ldots & 0 \\ -L_1 C_d & 0 & A_d & \ldots & 0 \\ \vdots & \vdots & \vdots & & \vdots \\ -L_n C_d & \ldots & \ldots & \ldots & A_d \end{bmatrix} \Xi_k - \begin{bmatrix} L_0 \\ L_1 \\ L_2 \\ \vdots \\ L_n \end{bmatrix} diag \left(\tilde{D}(x_k) \right)_{n+1} \end{aligned} \tag{20}$$

Define the coefficient matrix E_{n+1} and $\mathcal{L}_{n+1}$ as follows:

$$E_{n+1} = \begin{bmatrix} A_d - L_0 C_d & I & 0 & \ldots & 0 \\ -L_1 C_d & A_d & I & \ldots & 0 \\ -L_2 C_d & 0 & A_d & \ldots & 0 \\ \vdots & \vdots & \vdots & & \vdots \\ -L_n C_d & \ldots & \ldots & \ldots & A_d \end{bmatrix}, \quad \mathcal{L}_{n+1} = \begin{bmatrix} L_0 \\ L_1 \\ L_2 \\ \vdots \\ L_n \end{bmatrix} \tag{21}$$

The derivative of error vector we defined can eventually be written in the following form

$$\Xi_{k+1} = E_{n+1} \Xi_k - \mathcal{L}_{n+1} diag \left(\tilde{D}(x_k) \right)_{n+1} \tag{22}$$

Remark 3.1. *By the definition of Equation (22), the main problem is changed from the high-order disturbance observer designed to choose proper parameters to make sure that dynamic (22) converges to a bounded interval.*

3.3. **Stability analysis.** According to the systems we established in this paper, the following theorem holds.

Theorem 3.1. *Consider a quadrotor system defined in Equation (1) under the disturbance dynamic defined in Equation (2) under Assumptions 2.1, 2.2, and 2.3. The GRNN is defined as Equations (6)-(12), the HODO is defined as Equations (16) and (18), and the parameters will be chosen properly such that the system is UUB.*

Proof: According to the previous discussion, we can have the estimation error of GRNN based on Equation (12) and the estimation error of HODO defined in Equation (22). To prove the stability of the whole system, the Lyapunov function can be chosen as the following form:

$$V_k = \Xi_k^T P \Xi_k + \tilde{\Phi}_k^T \tilde{\Phi}_k + \tilde{y}_k^T \tilde{y}_k \tag{23}$$

For the first part, we can have the derivative in the form of

$$\begin{aligned}
\Delta V_{1_{k+1}} &= \Xi_{k+1}^T P \Xi_{k+1} - \Xi_k^T P \Xi_k \\
&= (E_{n+1}\Xi_k - \mathcal{D}_k)^T (E_{n+1}\Xi_k - \mathcal{D}_k) - \Xi_k^T P \Xi_k \\
&= \Xi_k^T \left(E_{n+1}^T P E_{n+1} - P\right) \Xi_k + \mathcal{D}_k^T P \mathcal{D}_k + 2\mathcal{D}_k^T P E_{n+1} \Xi_k
\end{aligned} \tag{24}$$

where $\mathcal{D}_k := -\mathcal{L}_{n+1} diag\left(\tilde{D}(x_k)\right)_{n+1}$ for the convenience of writing. Furthermore, by introducing Young's inequality, we can obtain

$$\begin{aligned}
\Delta V_{1_{k+1}} &\leq \Xi_k^T \left(E_{n+1}^T P E_{n+1} - P\right) \Xi_k + \mathcal{D}_k^T P \mathcal{D}_k + \Xi_k^T E_{n+1}^T P^T P E_{n+1} \Xi_k + \mathcal{D}_k^T I \mathcal{D}_k \\
&\leq \Xi_k^T \left[E_{n+1}^T P E_{n+1} + (P E_{n+1})^T (P E_{n+1}) - P\right] \Xi_k + \mathcal{D}_k^T (P + I) \mathcal{D}_k
\end{aligned} \tag{25}$$

Introducing Equation (12) and Young's inequality, we can obtain

$$\begin{aligned}
\Delta V_{2_{k+1}} &= \tilde{\Phi}_{k+1}^T \tilde{\Phi}_{k+1} - \tilde{\Phi}_k^T \tilde{\Phi}_k \\
&= \left(\hat{\Phi}_k - \gamma \Theta_n(x_k) \tilde{y}_k\right)^T \left(\hat{\Phi}_k - \gamma \Theta_n(x_k) \tilde{y}_k\right) - \tilde{\Phi}_k^T \tilde{\Phi}_k \\
&= \gamma^2 \tilde{y}_k^T \Theta_n(x_k)^T \Theta_n(x_k) \tilde{y}_k - 2\gamma \tilde{\Phi}_k^T \Theta_n(x_k) \tilde{y}_k^T \\
&\leq \tilde{\Phi}_k^T \tilde{\Phi}_k - 2\gamma^2 \mu^2 \tilde{y}_k^T \tilde{y}_k
\end{aligned} \tag{26}$$

According to the conclusion of [13], the following lemma holds.

Lemma 3.1. *The tracking error $\tilde{y}_{k+1}$ at time $k+1$ can be expressed as*

$$\tilde{y}_{k+1} \leq \tilde{y}_k - B \tag{27}$$

where $B = [\beta_1, \beta_2, \ldots, \beta_n]^T$, and for $i = 1, 2, \ldots, n$, β_i is a positive constant.

Then last part of ΔV yields

$$\begin{aligned}
\Delta V_{3_{k+1}} &= \tilde{y}_{k+1}^T \tilde{y}_{k+1} - \tilde{y}_k^T \tilde{y}_k \\
&\leq (\tilde{y}_k - B)^T (\tilde{y}_k - B) - \tilde{y}_k^T \tilde{y}_k \\
&\leq \tilde{y}_k^T \tilde{y}_k - 2B^T B
\end{aligned} \tag{28}$$

Finally, by introducing Equations (26), (27), and (28) into (24), we can get the derivative form of the total Lyapunov function as

$$\begin{aligned}
\Delta V_{k+1} &\leq \Xi_k^T \left[E_{n+1}^T P E_{n+1} + (P E_{n+1})^T (P E_{n+1}) - P\right] \Xi_k + \mathcal{D}_k^T (P + I) \mathcal{D}_k + \tilde{\Phi}_k^T \tilde{\Phi}_k \\
&\quad - 2\gamma^2 \mu^2 \tilde{y}_k^T \tilde{y}_k + \tilde{y}_k^T \tilde{y}_k - 2B^T B \\
&\leq \Xi_k^T \left[E_{n+1}^T P E_{n+1} + (P E_{n+1})^T (P E_{n+1}) - P\right] \Xi_k + \left(1 - 2\gamma^2 \mu^2\right) \tilde{y}_k^T \tilde{y}_k - 2B^T B
\end{aligned} \tag{29}$$

According to Schur's Complement Lemma, we can write the matrix of the first term as

$$\begin{bmatrix} -P & (PE_{n+1})^T & (PE_{n+1})^T \\ * & -P & 0 \\ * & * & -I \end{bmatrix} \leq 0 \tag{30}$$

We can use the LMI toolbox in Matlab to solve L to make Equation (30) established. Together with $1-2\gamma^2\mu^2 \leq 0$, we know that the Lyapunov function of the system is UUB.

4. **Simulation Example.** A numerical simulation example of the quadrotor is discussed in this section to demonstrate the effectiveness of the HODO and GRNN designed in this paper. According to the quadrotor model given in Equation (1), the disturbance is presented as

$$\begin{cases} \xi_{k+1} = \begin{bmatrix} 1 & 0 & 0 \\ 0 & 1 & 0 \\ 0 & 0 & 0 \end{bmatrix} \xi_k \\ d_k = \begin{bmatrix} 1 & 0 & 0 \\ 0 & 1 & 0 \\ 0 & 0 & 0 \end{bmatrix} \xi_k + \begin{bmatrix} 1.5\sin t \\ 1.5\sin t \\ 0 \end{bmatrix} \end{cases} \tag{31}$$

The reference signal is defined in the continuous-time zone as $r = \left[15\sin\left(\frac{1}{25}t\right), 15\sin\left(\frac{1}{25}t + \frac{\pi}{2}\right), 0.5t\right]^T$ with the sampling interval is set to $T = 0.05$ s. The numerical simulation results are shown in Figures 1 and 2.

Figure 1 shows the states of the position tracking signal under the three coordinate axes. It can be seen from the figure that the system output can track the reference signal

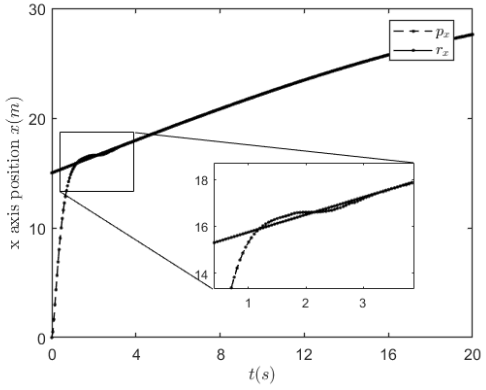

(a) x-axis tracking response

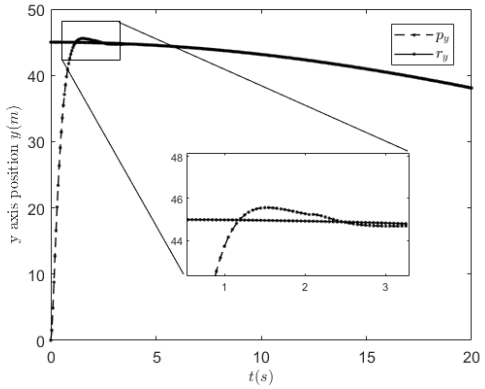

(b) y-axis tracking response

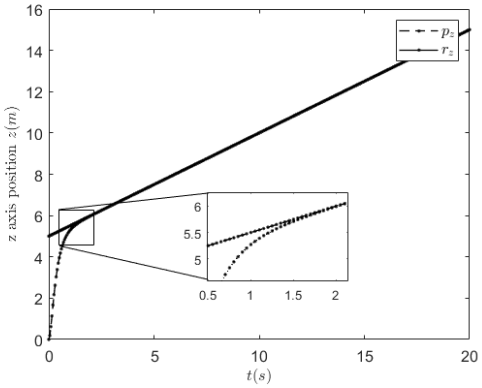

(c) z-axis tracking response

FIGURE 1. Tracking response of the position

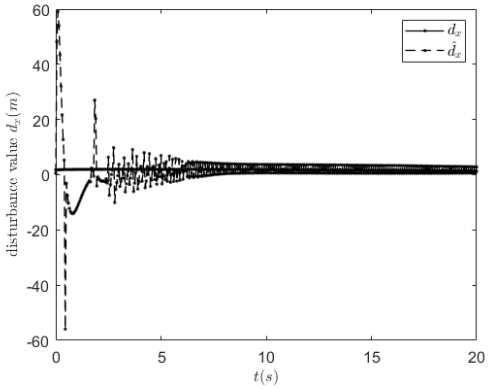

(a) x-axis observer comparison

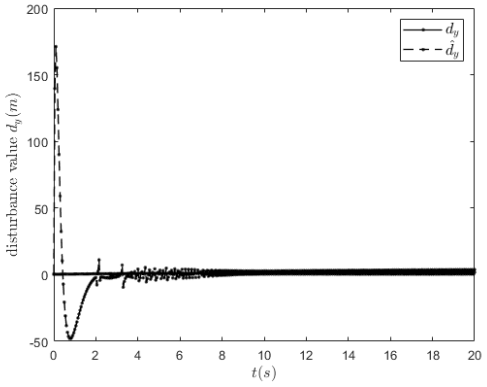

(b) y-axis observer comparison

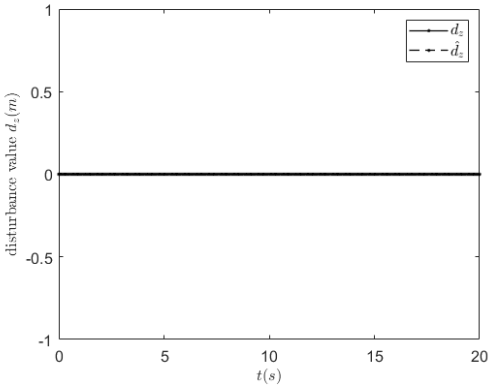

(c) z-axis observer comparison

FIGURE 2. Disturbance observer compensation in three axes

well in three directions. Figure 2 shows the estimation of the disturbances. Since no additional disturbance is applied in the z direction, the estimated and actual values stay zero. However, the estimated value of disturbance in the x and y axes varies in the region due to the estimation error brought by the high-order disturbance observer within the set interval. The effectiveness of the algorithm designed in this paper can be concluded from analyzing the experimental results.

5. **Conclusion.** In this work, a new disturbance model has been established to ensure that the flight of QUAVs in large buildings is not disturbed by wind and turbulence. In order to better estimate the nonlinear turbulence, a GRNN has been designed to estimate the nonlinear part of the disturbance, and for the linear part an HODO has been designed to ensure the stability of the system. Finally, by defining the Lyapunov function and using Schur's complement lemma to solve the parameters can keep the system UUB. The work will further move on to embedded model control and its usage on this system to improve the performance of the control system.

Acknowledgment. This work is partially supported by the Postgraduate Research & Practice Innovation Program of Jiangsu Province under Grant KYCX23_0386, the National Science Fund for Distinguished Young Scholars under Grant 61825302 and the Jiangsu Province Postdoctoral Science Foundation under Grant 2020Z112. The authors also gratefully acknowledge the helpful comments and suggestions of the reviewers, which have improved the presentation.

REFERENCES

[1] F. Luo et al., A distributed gateway selection algorithm for QUAV networks, *IEEE Transactions on Emerging Topics in Computing*, vol.3, no.1, pp.22-33, 2015.

[2] V. A. Azarov et al., Composite 3D printing for the small size unmanned aerial vehicle structure, *Composites Part B: Engineering*, vol.169, pp.157-163, 2019.

[3] Z. Wang, Q. Gao, J. Xu et al., A review of UAV power line inspection, *Proc. of 2020 International Conference on Guidance, Navigation and Control*, Tianjin, China, pp.3147-3159, 2022.

[4] C. Liu and T. Szirányi, Road condition detection and emergency rescue recognition using on-board UAV in the wildness, *Remote Sensing*, vol.14, no.17, 4355, 2022.

[5] Z. Jiao, Y. Zhang, J. Xin et al., A deep learning based forest fire detection approach using UAV and YOLOv3, *The 1st International Conference on Industrial Artificial Intelligence*, pp.1-5, 2019.

[6] B. B. Kocer et al., Inspection-while-flying: An autonomous contact-based nondestructive test using QUAV-tools, *Automation in Construction*, vol.106, 102895, 2019.

[7] J. Huang, M. Zhang, S. Ri, C. Xiong, Z. Li and Y. Kang, High-order disturbance-observer-based sliding mode control for mobile wheeled inverted pendulum systems, *IEEE Transactions on Industrial Electronics*, vol.67, no.3, pp.2030-2041, 2020.

[8] S. Shao, M. Chen and Y. Zhang, Adaptive discrete-time flight control using disturbance observer and neural networks, *IEEE Transactions on Neural Networks and Learning Systems*, vol.30, no.12, pp.3708-3721, 2019.

[9] S. Phukapak, D. Koyama, K. Hashikura, M. A. S. Kamal and K. Yamada, The parameterization of all disturbance observers for periodic output disturbances, *International Journal of Innovative Computing, Information and Control*, vol.19, no.1, pp.163-180, 2023.

[10] S. Shao, M. Chen and Y. Zhang, Adaptive discrete-time flight control using disturbance observer and neural networks, *IEEE Transactions on Neural Networks and Learning Systems*, vol.30, no.12, pp.3708-3721, 2019.

[11] B. Sarsembayev, K. Suleimenov and T. D. Do, High order disturbance observer based PI-PI control system with tracking anti-windup technique for improvement of transient performance of PMSM, *IEEE Access*, vol.9, pp.66323-66334, 2021.

[12] N. Ahmed, M. Chen and S. Shao, Disturbance observer based tracking control of quadrotor with high-order disturbances, *IEEE Access*, vol.8, pp.8300-8313, 2020.

[13] A. J. Al-Mahasneh, S. G. Anavatti, M. A. Garratt and M. Pratama, Stable adaptive controller based on generalized regression neural networks and sliding mode control for a class of nonlinear time-varying systems, *IEEE Transactions on Systems, Man, and Cybernetics: Systems*, vol.51, no.4, pp.2525-2535, 2021.

[14] F. Rinaldi, S. Chiesa and F. Quagliotti, Linear quadratic control for quadrotors UAVs dynamics and formation flight, *Journal of Intelligent & Robotic Systems*, vol.70, pp.203-220, 2013.